Supplemental Figures

SI Fig 1. Characterization of 29 ASD/NDD rare variant target genes.

SI Fig 2. ASD pooled scCRISPR-KO screen validation.

SI Fig 3. ASD scCRISPR-KO screen in hiPSC derived iNPCs, iGLUTs, and iGABAs.

SI Fig 4. Seurat single-cell CRISPR screen QC, cell population heterogeneity quantification, demultiplexing, and covariate selection in iNPCs.

SI Fig 5. Seurat single-cell CRISPR screen QC, cell population heterogeneity quantification, demultiplexing, and covariate selection in immature iGLUTs.

SI Fig 6. Seurat single-cell CRISPR screen QC, cell population heterogeneity quantification, demultiplexing, and covariate selection in mature iGLUTs.

SI Fig 7. Seurat single-cell CRISPR screen QC, cell population heterogeneity quantification, demultiplexing, and covariate selection in mature iGABAs.

SI Fig 8. Concordance between single-cell and pseudobulk differential gene expression analysis.

SI Fig 9. Correlations between hiPSC-derived cell types, zebrafish brain, and the adult and fetal brain.

SI Fig 10. Gene Ontology gene set enrichments and functional similarity between individual KOs across cell-types.

SI Fig 11. Rare variant ASD eGene KO phenotypes show low-level transcriptomic convergence across cell-types and developmental time points enriched in unique biological pathways.

SI Fig 12. Gene-level convergence across 9 KOs is unique across cell-types and increases with maturity in iGLUT neurons.

SI Fig 13. Gene-level and network-level convergence across 21 KOs in iGLUT and iGABA neurons.

SI Fig 14. miRNA targets converge on unique networks in iNPCs, immature and mature iGLUTs, and mature iGABAs.

SI Fig 15. Random forest training data characteristics and node frequency across trees.

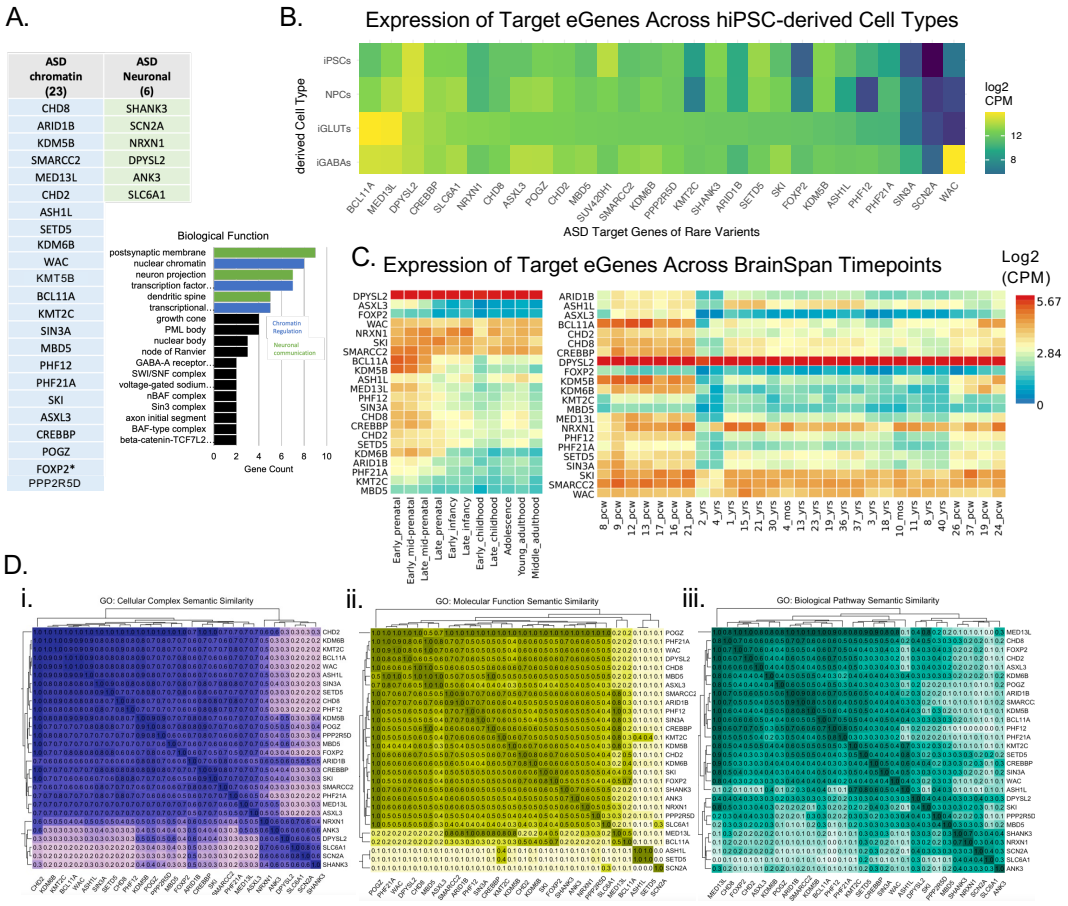

SI Fig 1. Characterization of 29 ASD/NDD rare variant target genes. (A) Broad functional classification of genes selected for ASD scCRISPR-KO pool screen. **(B)** Bulk RNA-seq heatmap of selected 29 ASD risk genes expression in hiPSCs, NPCs, iGLUTs, iGABAs. **(C)** Normalized log2(CPM) of 29 ASD risk genes across BrainSpan developmental stages pulled using FUMA**. (D)** Semantic similarity between 29 ASD risk genes for membership in Gene Ontology (GO) functional cellular component, biological process, and molecular function gene sets

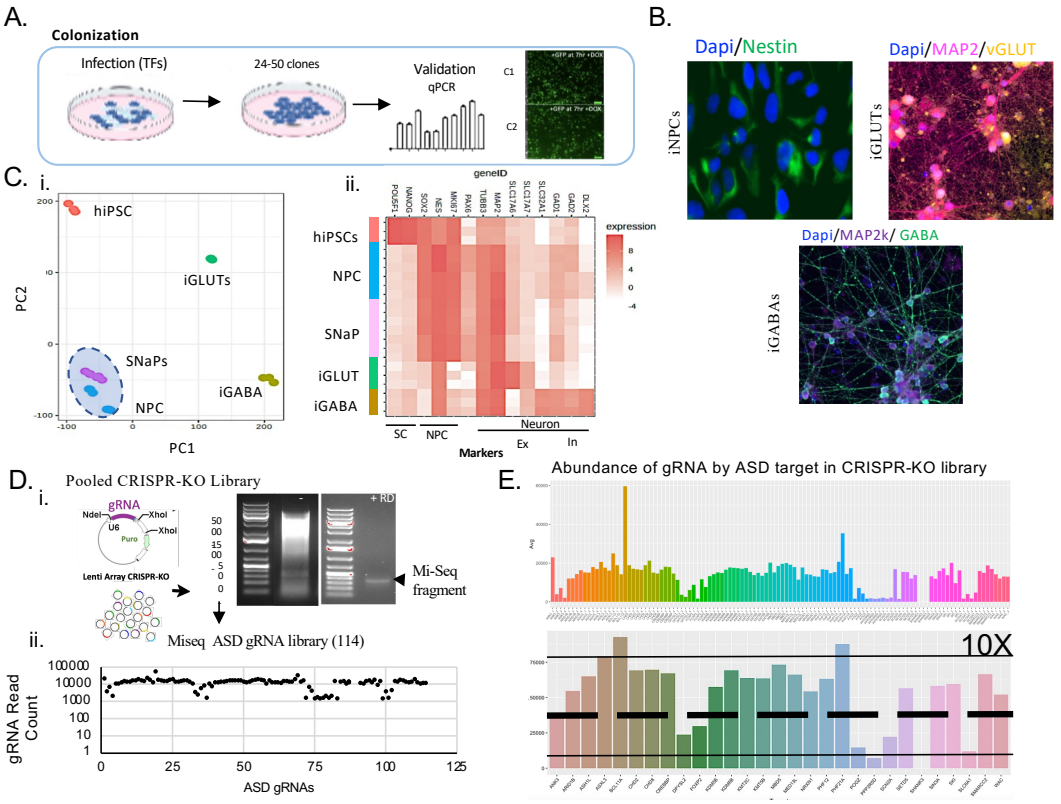

SI Fig 2. ASD pooled scCRISPR-KO screen validation. (A) Illustration of clonalization process for NPC, iGLUT, and iGABA lines used in the scCRISPR-KO screens. **(B)** Immuohistochemistry of cell-type-specific markers in iNPCs (NESTIN, green), iGLUTs (MAP2, pink; vGLUT, yellow), iGABAs (MAP2, purple; GABA, green). **(C)** Characterization of gene expression in hiPSCs, NPCs/SNaPs, iGLUTs, and iGABAs by **(i)** PCA and **(ii)** average expression of cell-type specific markers. **(D)** Diagram of the gRNA plasmid insertion site and gel electrophoresis of cloned pooled library restriction digested (RD) for Mi-seq validation. **(E)** Frequency of ASD pooled gRNA (counts) in library by Mi-seq.

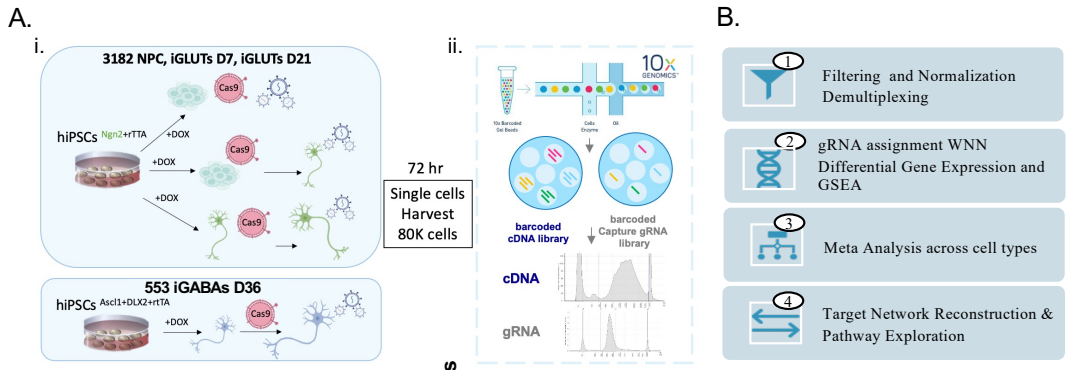

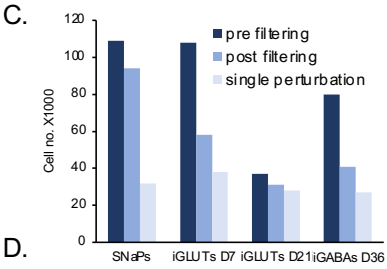

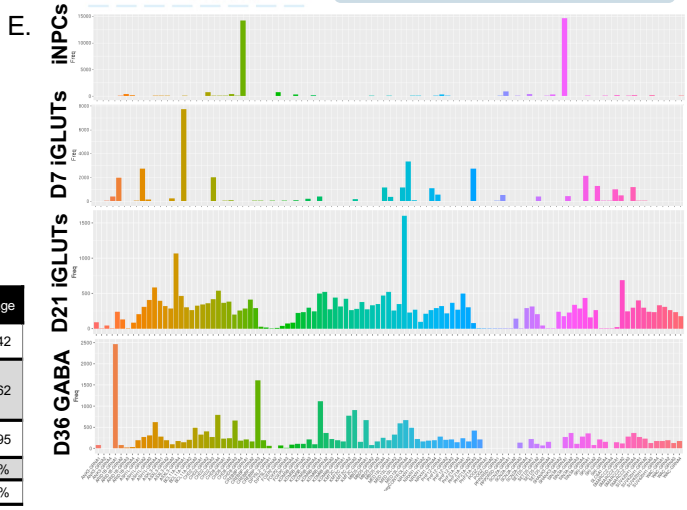

D.

	iNPCs	D7 iGLUT	D21 iGLUT	D36 iGABA	Average
# of cells (pre-filter)	108,616	108,077	36,722	79,834	98,842
# of cells post-filtering & removal of negatives	94,363	57,685	31,473	41,340	64,462
# of singlets retained	35,240	38,097	28,388	26,549	33,295
% doublets	62.7%	34%	9.8%	35.8%	48.3%
% singlets	37.3%	66%	90.2%	64.2%	51.7%

SI Fig 3. ASD scCRISPR-KO screen in hiPSC-derived iNPCs, iGLUTs, and iGABAs. (A) Illustration scCRISPR-KO screen experimental set-up. Note iNPCs and iGLUTs in control 1 (3182-3-clone5) and iGABAs in control 2 (553-3-clone34). **(B)** Analytical process following 10x sequencing. **(C)** Number of cells sequences (pre-filtering), post-filtering, and post selection for single gRNA demultiplexing across cell-types. **(D)** Table of number of cells – including percent singlets and doublets by experiment. **(E)** Frequency of cell gRNA identity by experiment.

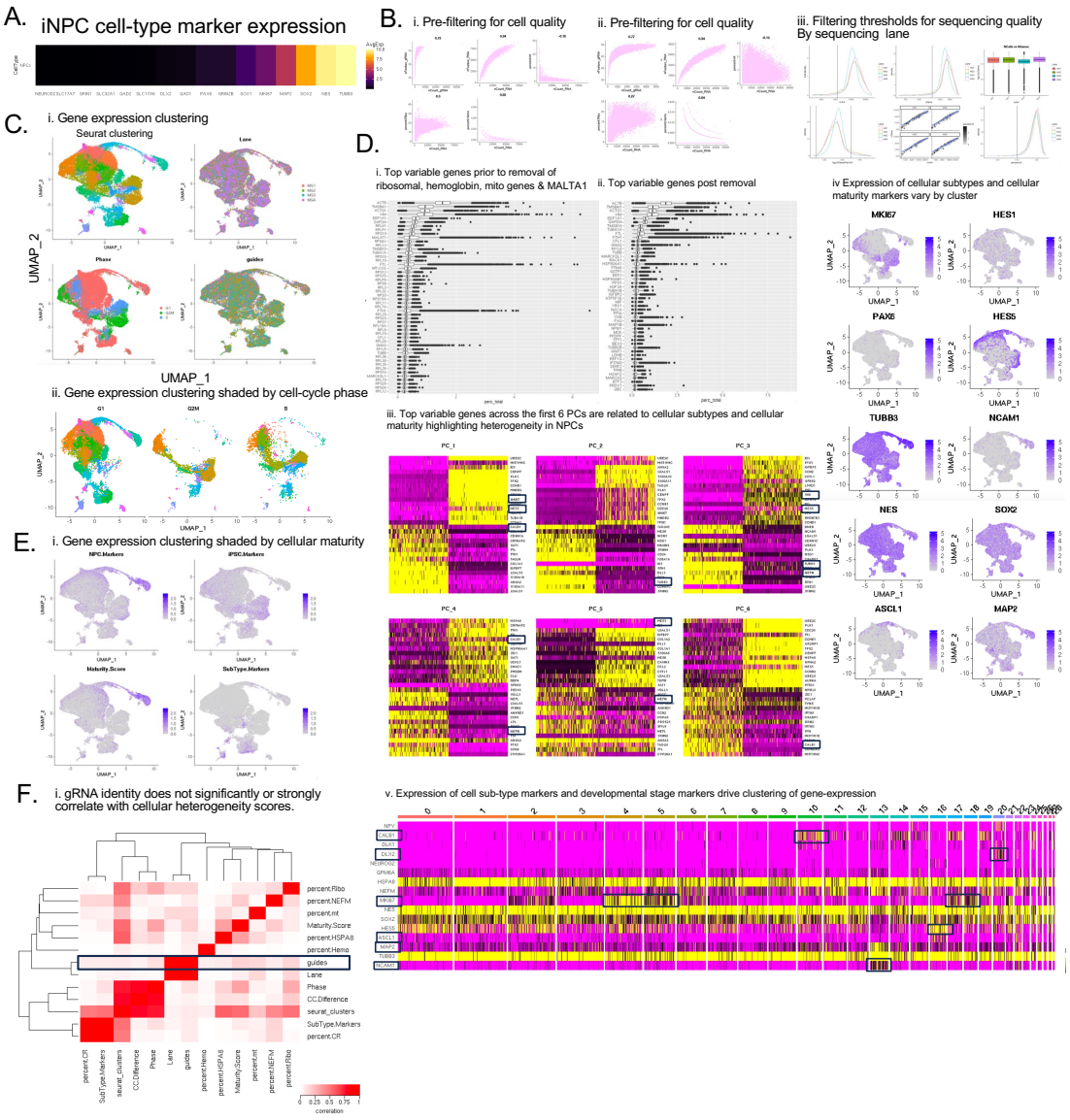

SI Figure 4. Seurat single-cell CRISPR screen QC, cell population heterogeneity quantification, demultiplexing, and covariate selection in iNPCs. (**A**) NPC cell-type marker expression confirms the cellular identity as NPCs. **(B)** Pre- and post-filtering distribution of cells by quality controls metrics including mitochondrial gene percent expression and read depth. **(C)** Expression single-cell based clustering with UMAP dimensionality reduction colored by Seurat cluster, lane, cell-cycle phase (see also ii), or gRNA identity (guide). **(D)** Top genes driving variance between clusters are related to ribosomal or mitochondrial genes, as well long transcript genes that are often variable in single-cell sequencing; **(ii)** after removal of ribosomal, hemoglobin, mitochondrial genes as well as MALTA1 top genes driving variance between clusters are related to cellular maturity and cellular subtype markers. **(iii)** Top variable genes across the first 6 PCs are related to cellular subtypes and cellular maturity highlighting heterogeneity in NPCs. **(iv)** Expression of cellular subtypes and cellular maturity markers vary by cluster. **(v)** Expression of cell sub-type markers and developmental stage markers drive clustering of gene-expression **(E)** Distribution of maturity, cell-phase, and cellular-subtype scores based on UMAP clustering identifies clustering driven by cellular heterogeneity. (**F**) This cellular heterogeneity is not significantly, or strongly, correlated with gRNA identity and was included as a covariate to correct for in the SCTransform normalization.

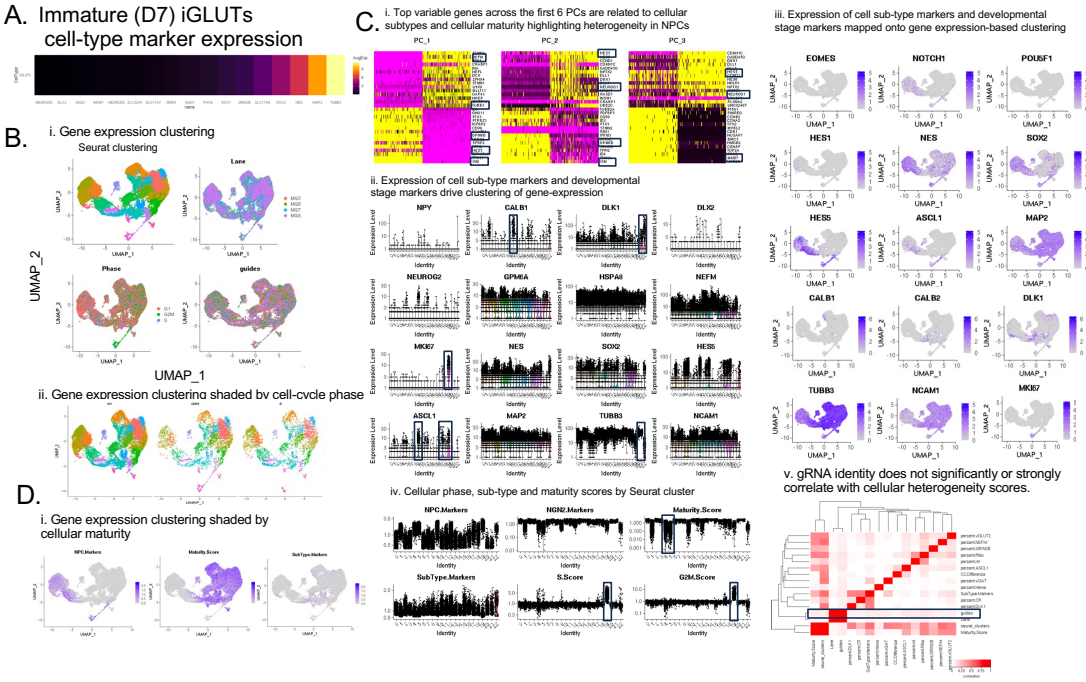

SI Figure 5. Seurat single-ell CRISPR screen QC, cell population heterogeneity quantification, demultiplexing, and covariate selection immature (D7 iGLUTs). **(A)** Cell-type marker expression confirms the cellular identity as glutamatergic neurons. **(B)** Expression based single-cell based clustering with UMAP dimensionality reduction colored by Seurat cluster, lane, cell-cycle phase (see also ii), or gRNA identity (guide). **(C) (i)** Top variable genes across the first 3 PCs are related to cellular subtypes and cellular maturity highlighting heterogeneity. **(iii)** Expression of cell sub-type markers and developmental stage markers drive clustering of gene-expression. **(iii)** Expression of cell sub-type markers and developmental stage markers mapped onto gene expression-based clustering. **(iv)** Cellular phase, sub-type and maturity scores by Seurat cluster. **(v)** gRNA identity does not significantly or strongly correlate with cellular heterogeneity scores. **(D)** Distribution of maturity, cell-phase, and cellular-subtype scores based on UMAP clustering identifies clustering driven by cellular heterogeneity. Cellular heterogeneity was included as a covariate to correct for in the SCTransform normalization.

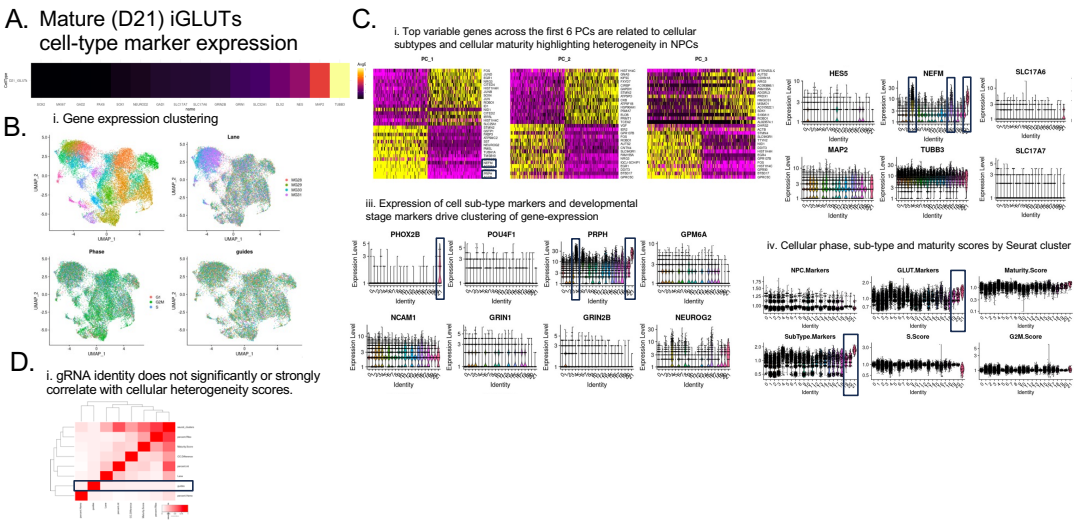

SI Figure 6. Seurat csingle-ell CRISPR screen QC, cell population heterogeneity quantification, demultiplexing, and covariate selection mature (D21 iGLUTs). **(A)** Cell-type marker expression confirms the cellular identity as glutamatergic neurons. **(B)** Expression based single-cell based clustering with UMAP dimensionality reduction colored by Seurat cluster, lane, cell-cycle phase (see also ii), or gRNA identity (guide). **(C) (i)** Top variable genes across the first 3 PCs are related to cellular subtypes and cellular maturity highlighting heterogeneity. **(iii)** Expression of cell sub-type markers and developmental stage markers drive clustering of gene-expression. **(iv)** Cellular phase, sub-type and maturity scores by Seurat cluster. **(D)** This cellular heterogeneity is not significantly, or strongly, correlated with gRNA identity and was included as a covariate to correct for in the SCTransform normalization.

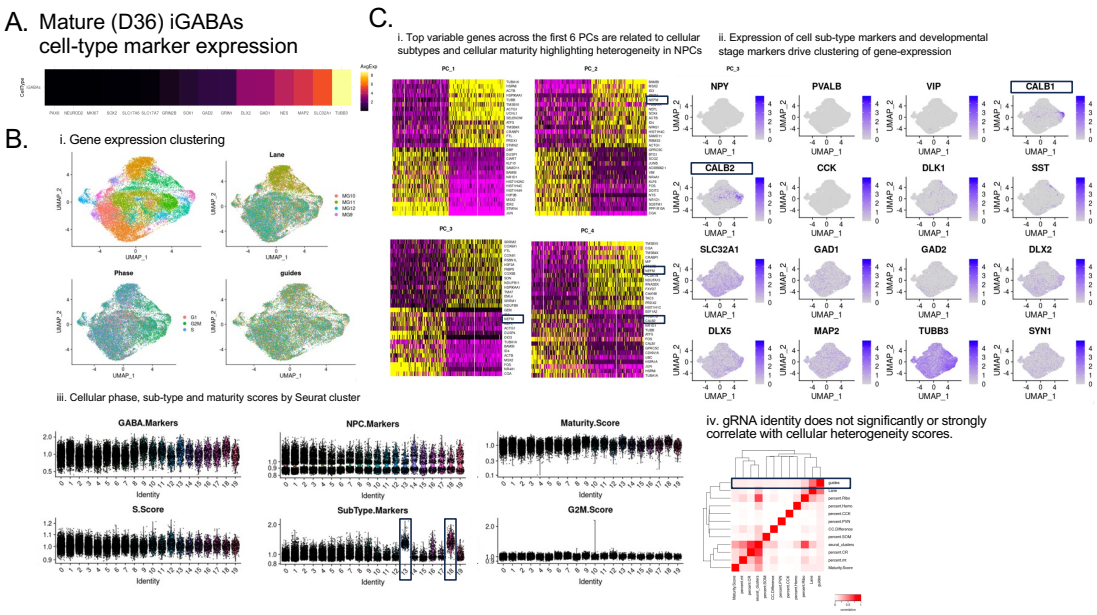

SI Figure 7. Seurat single-cell CRISPR screen QC, cell population heterogeneity quantification, demultiplexing, and covariate selection mature (D36 iGABAs). **(A)** Cell-type marker expression confirms the cellular identity as GABAergic neurons. **(B)** Expression based single-cell based clustering with UMAP dimensionality reduction colored by Seurat cluster, lane, cell-cycle phase (see also ii), or gRNA identity (guide). **(C) (i)** Top variable genes across the first 4 PCs are related to cellular subtypes and cellular maturity highlighting heterogeneity in NPCs. **(ii)** Expression of cell sub-type markers and developmental stage markers drive clustering of gene-expression. **(iii)** Cellular phase, sub-type and maturity scores by Seurat cluster. **(iv)** This cellular heterogeneity is not significantly, or strongly, correlated with gRNA identity and was included as a covariate to correct for in the SCTransform normalization.

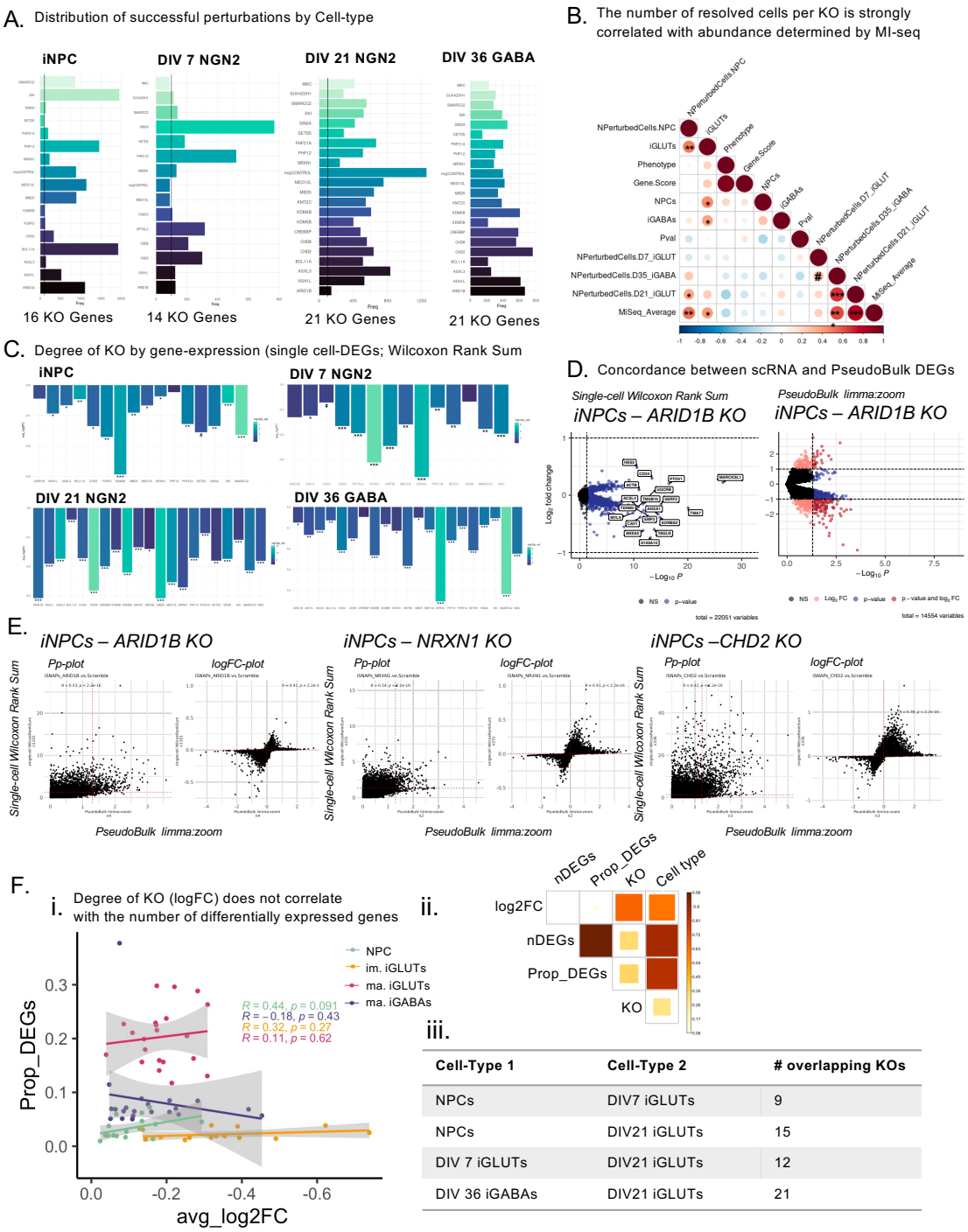

Cell-Type 1	Cell-Type 2	# overlapping KOs
NPCs	DIV7 iGLUTs	9
NPCs	DIV21 iGLUTs	15
DIV 7 iGLUTs	DIV21 iGLUTs	12
DIV 36 iGABAs	DIV21 iGLUTs	21

SI Fig 8. Concordance between single-cell and pseudobulk differential gene expression analysis. **(A)** Number of singlet cells by gRNA per cell-type **(B)** Correlations of the number of cells per gene target and the original distribution of gRNAs measured by Mi-seq shows that the final number of cell per guide significantly correlates with MiSeq abundance levels (**SI Table 3**). **(C)** Degree of logFC downregulation of target genes across cell-types. (D-E) Examples of the concordance of differential gene expression analysis using Wilcoxon Rank Sum test in single-cell data and limma:voom in pseudobulked data – **(D)** Volcano plots of differential gene expression in ARID1B KO versus non-targeting samples in NPCs. **(E)** Plots comparing p-values and logFC between differential gene expression analysis results at the single-cell level and pseudobulk level for ARID1B, NRXN1, and CHD2 (Pearson's correlation, Holm's adjusted P-values). **(F)** There was no significant correlation between the average logFC of the target KO gene and the final proportion of nominally significant DEGs in any cell-type (Pearson's correlation, Holm's adjusted P-values) **(i-ii). (iii)** The number of KOs successfully resolved shared between cell-types.- and thus allowing for direct comparison.

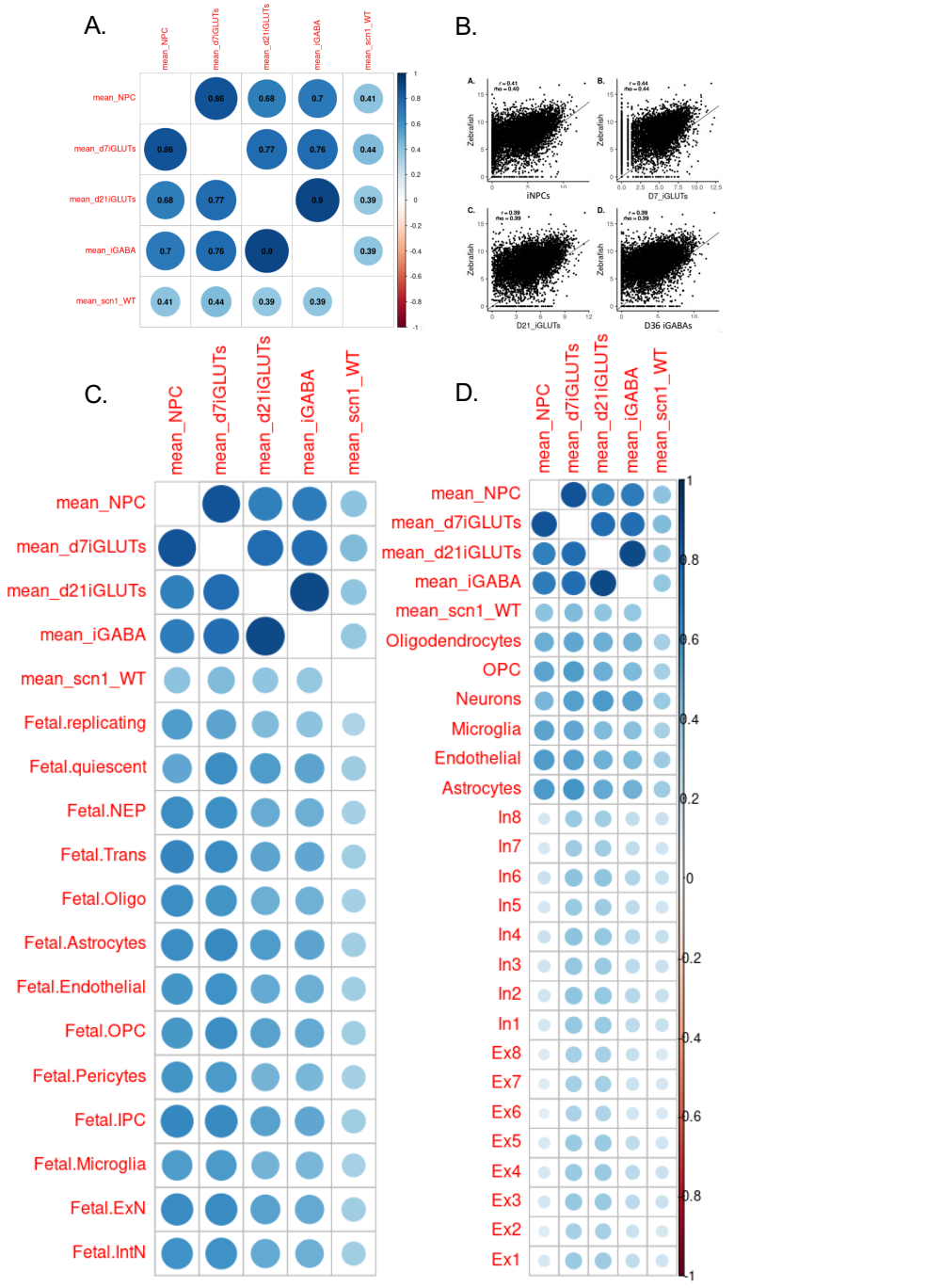

SI Fig 9. Correlations between hiPSC-derived cell types, zebrafish brain, and the adult and fetal brain. Expression of non-targeting cells in iNPCs, iGLUTs, and iGABAs significantly correlates with human fetal **(C)** and adult brain **(D)** expression and expression of gene homologs in the zebrafish brain **(A-B)**.

A. Gene Ontology gene-set enrichment analysis of individual KOs across cell-types

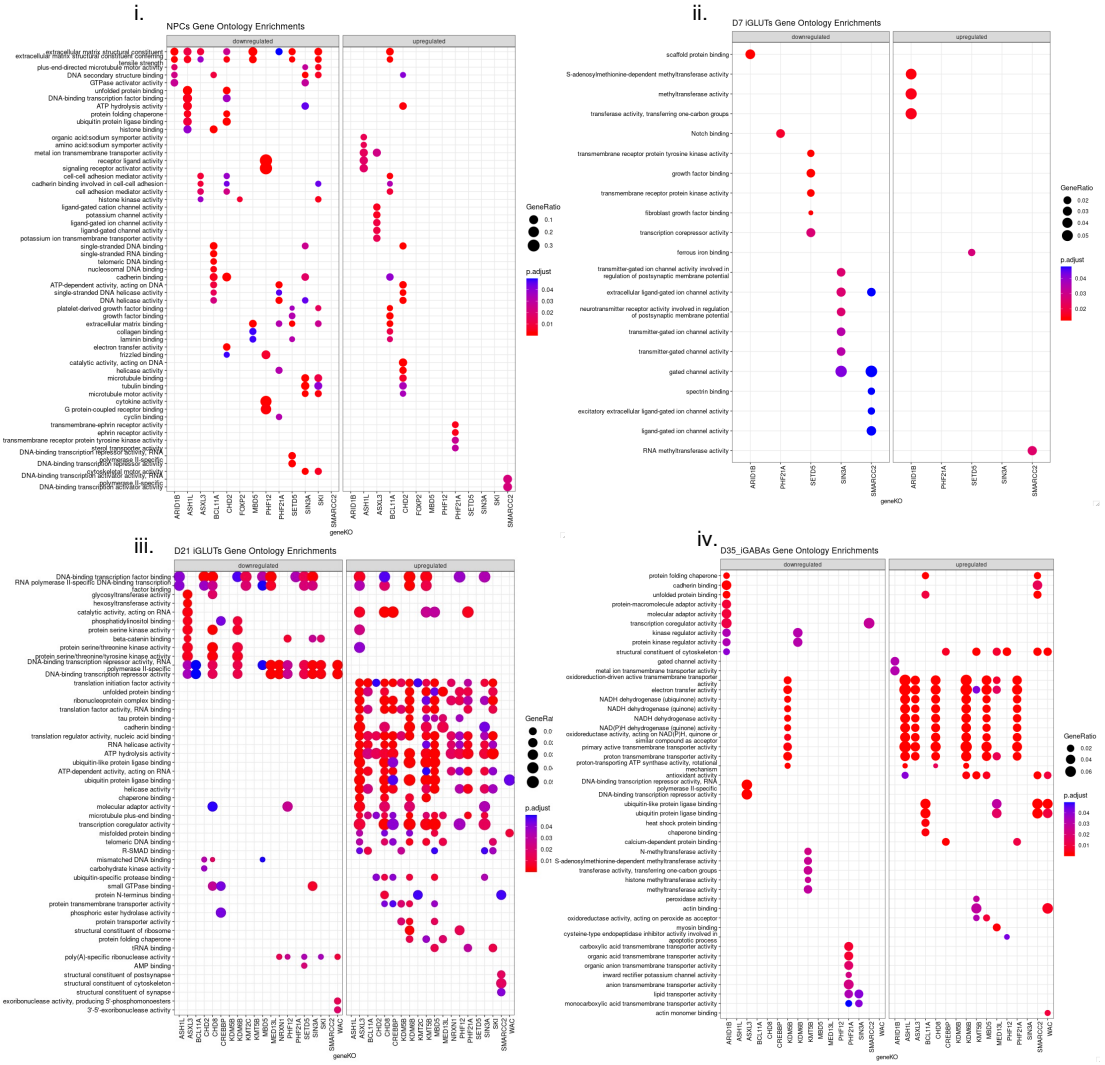

B. Biological Pathways – Semantic Similarity of DEG enrichments

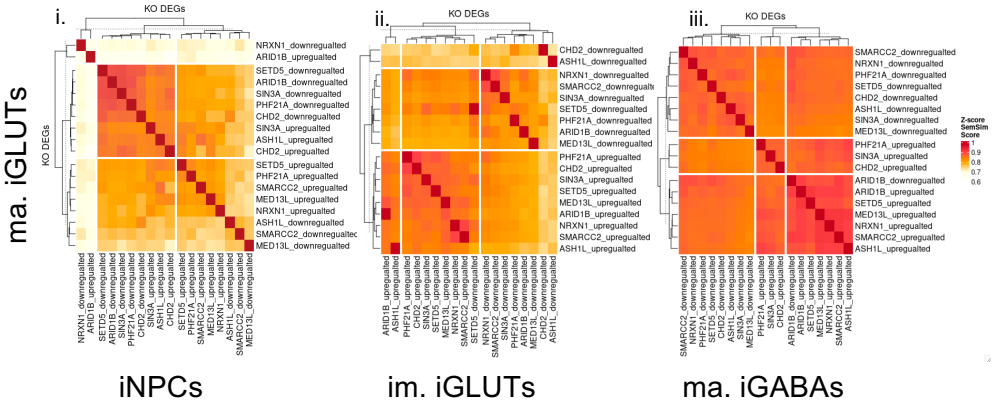

SI Fig 10. Gene Ontology (GO) gene set enrichments and functional similarity between individual KOs across cell-types. (A) GSEA results for GO geneset enrichments across (i) iNPCS, (ii) immature iGLUTs, **(ii)** mature iGLUTs, and **(iii)** mature iGABAs. **(B)** Semantic similarity of biological pathway membership of the significantly up and down-regulated DEGs for each KO compared across cells.

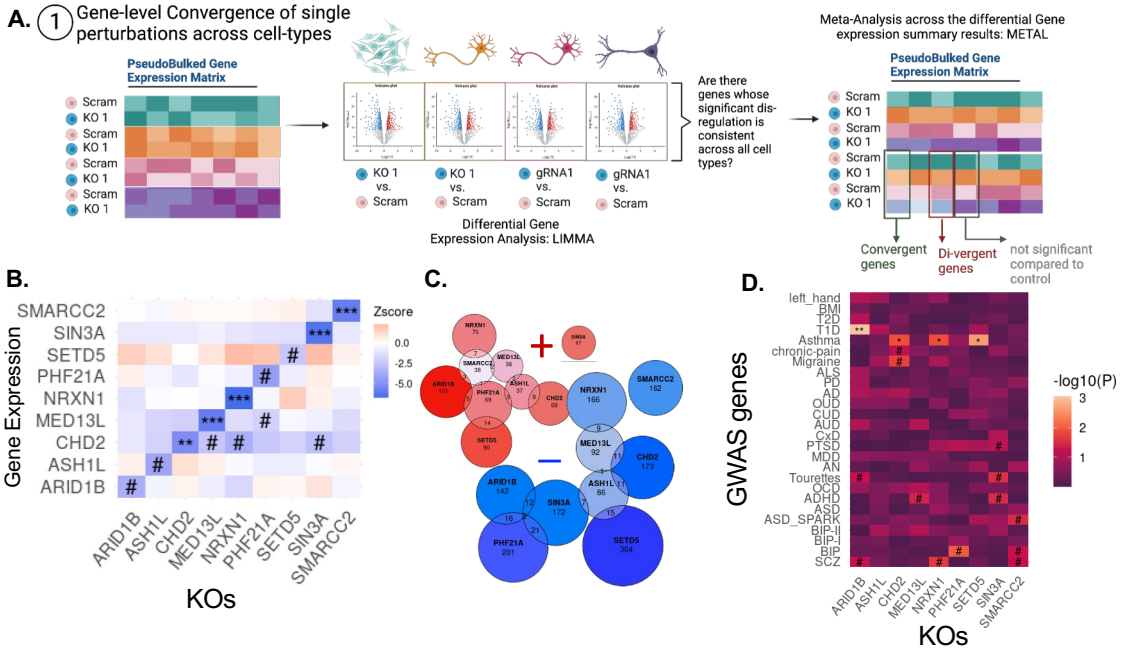

SI Fig 11. Rare variant ASD eGene KO phenotypes show low-level transcriptomic convergence across cell-types and developmental time points enriched in unique biological pathways. (A) Schematic explaining KO-specific cross cell-type convergence at the individual gene level using differential gene expression meta-analysis. **(B)** Heatmap of meta-analyzed z-score effects on gene expression of targeted KO eGenes across perturbation phenotypes (#, unadjusted p-value =<0.05, *FDR<=0.05, **FDR<0.01, ***FDR<0.001). **(C)** Euler diagrams of overlapping convergent genes by eGene KO phenotype (nominal p-value <=0.05; Cochran's Heterogeneity p-value > 0.05; positive (red) or (negative) direction of effect across all cell types). **(D)** Over representation analysis of KO-specific cross-cell type convergence and GWAS-risk associated genes.

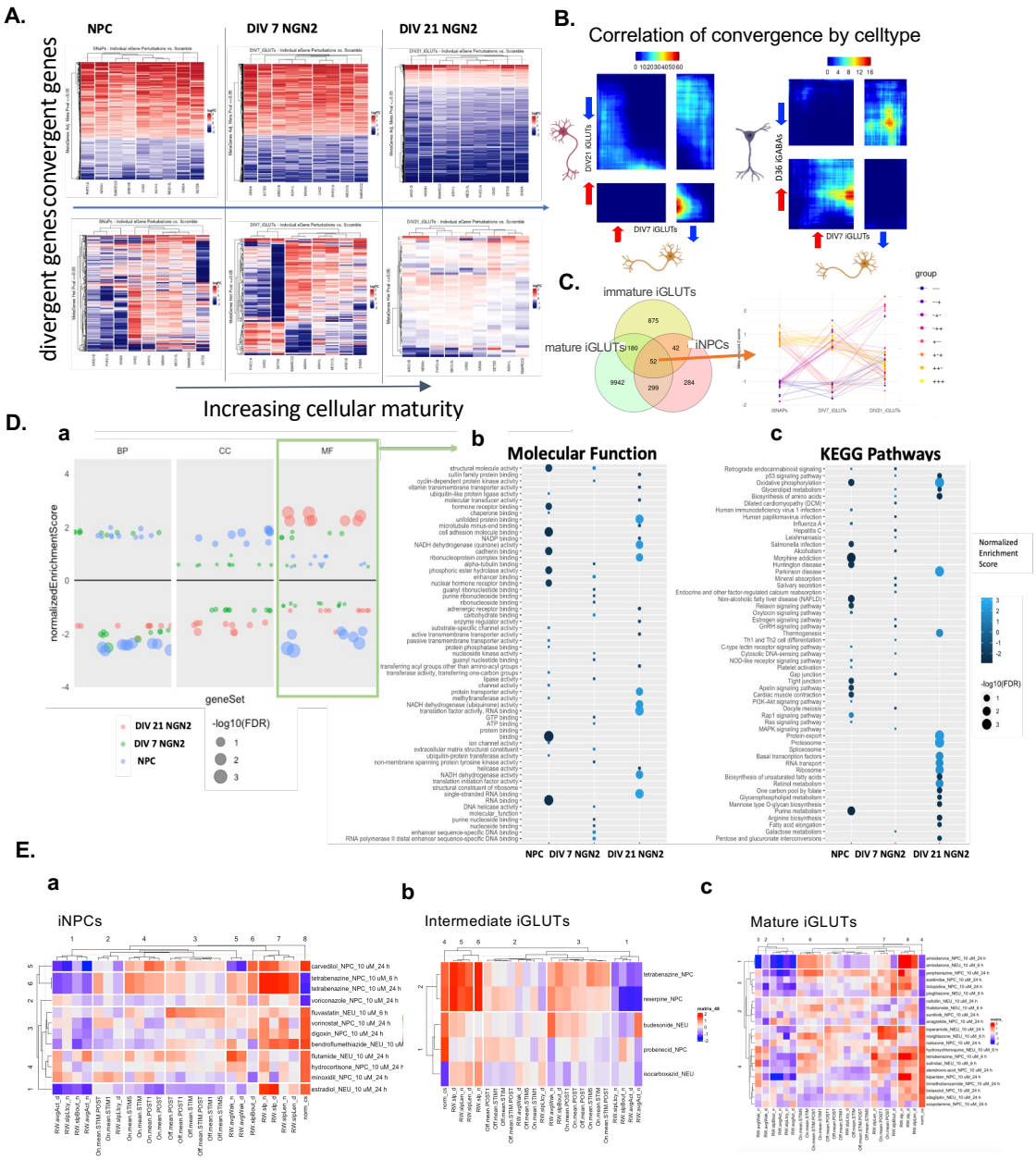

SI Fig 12. Gene-level convergence across 9 KOs is unique across cell-types and increases with maturity in iGLUT neurons. **(A)** Heatmaps of convergent and divergent genes across 9 individual KOs in NPCs, immature iGLUTs (DIV7 NGN2s), and mature neurons (DIV21 iGLUTs). **(B)** Comparison over transcriptomic wide meta pFDR and z-scores using RRHO correlation across mature neurons and immature iGLUTs. **(C) (i)** Overlap of convergent genes across NPCs, immature iGLUT, and mature iGLUTs and (ii) their direction of effect in each cell-type. **(D)** Broad Gene Ontology gene-set enrichment analysis of convergent genes across 9KOs **(b)** specific enrichments for molecular function and **(c)** KEGG pathway enrichments. **(E)** Behavioral phenotypic effects of top drugs predicted to mimic or reverse the convergent impact of 9 ASD KOs in **(a)** NPCs, **(b)** immature iGLUTs, and **(c)** mature iGLUTs.

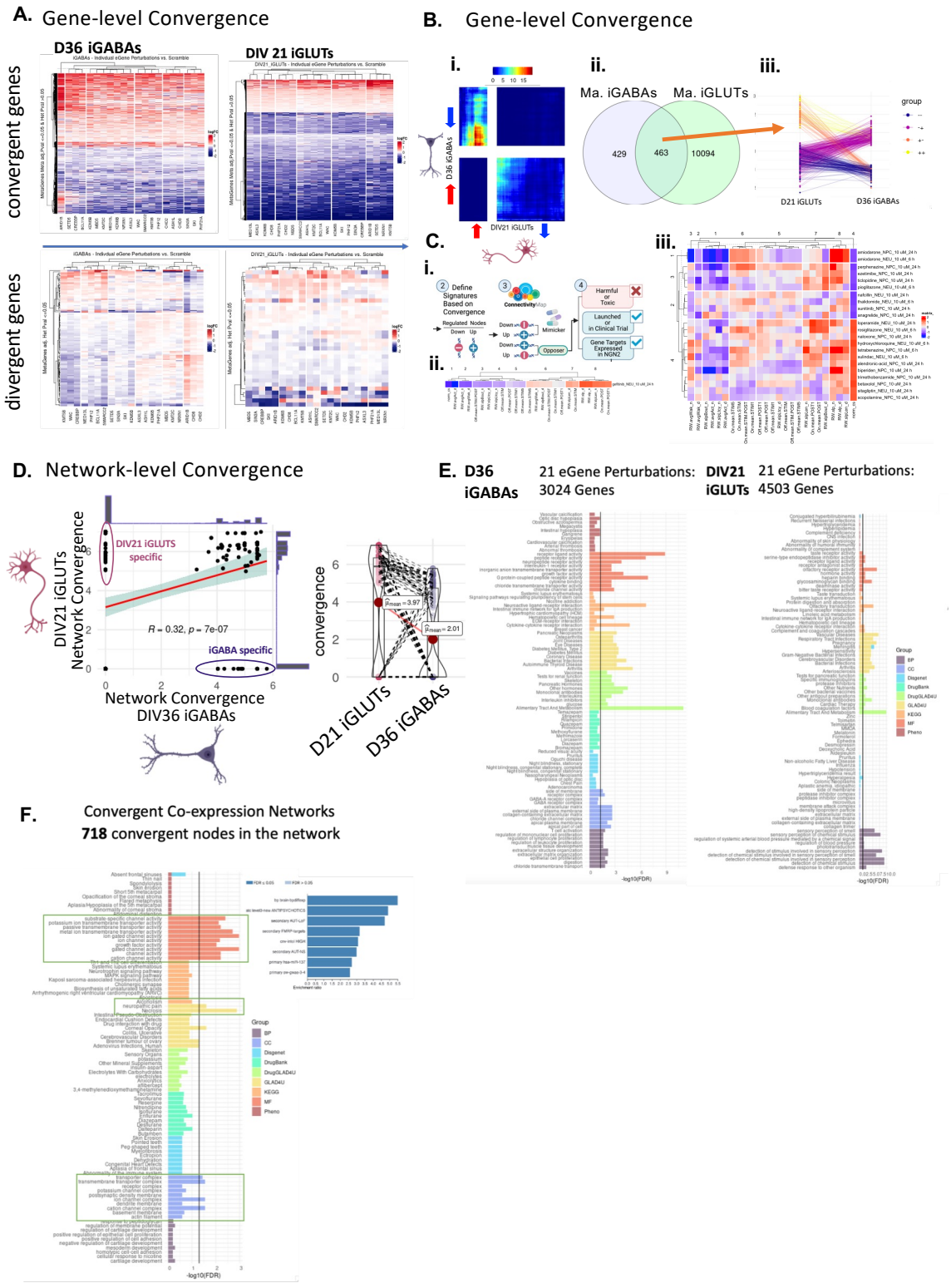

SI Fig 13. Gene-level and network-level convergence across 21 KOs in iGLUT and iGABA neurons. **(A)** Heatmaps of convergent and divergent genes across 9 individual KOs between mature iGLUTs and iGABAs. **(B)** **(i)** Comparison over transcriptomic wide meta pFDR and z-scores using RRHO correlation between mature iGLUTs and iGABAs. **(ii)** Overlap of convergent genes across mature iGLUTs and iGABAs and **(iii)** their direction of effect in each cell-type. **(C)** Behavioral phenotypic effects of top drugs predicted to mimic or reverse the convergent impact of 9 ASD KOs in **(i)** mature iGABAs and **(ii)** iGLUTs. **(D)** Comparison of the strength of network level convergence across different KO combinations – **(i)** While network convergence was generally strongly correlated between neuronal types, some cell-type specific networks exist and **(ii)** mature iGLUTs had significantly stronger mean convergence across all networks. **(E)** Gene set enrichment of convergent node genes shared across 21 KOs in iGLUTs and iGABAs identified unique function. **(F)** Exploration of cross KO network convergence shared across mature neurons identified a network of 718 genes enriched for synaptic signaling, channel signaling, neuropathic pain and rare and common psychotic risk associated gene targets.

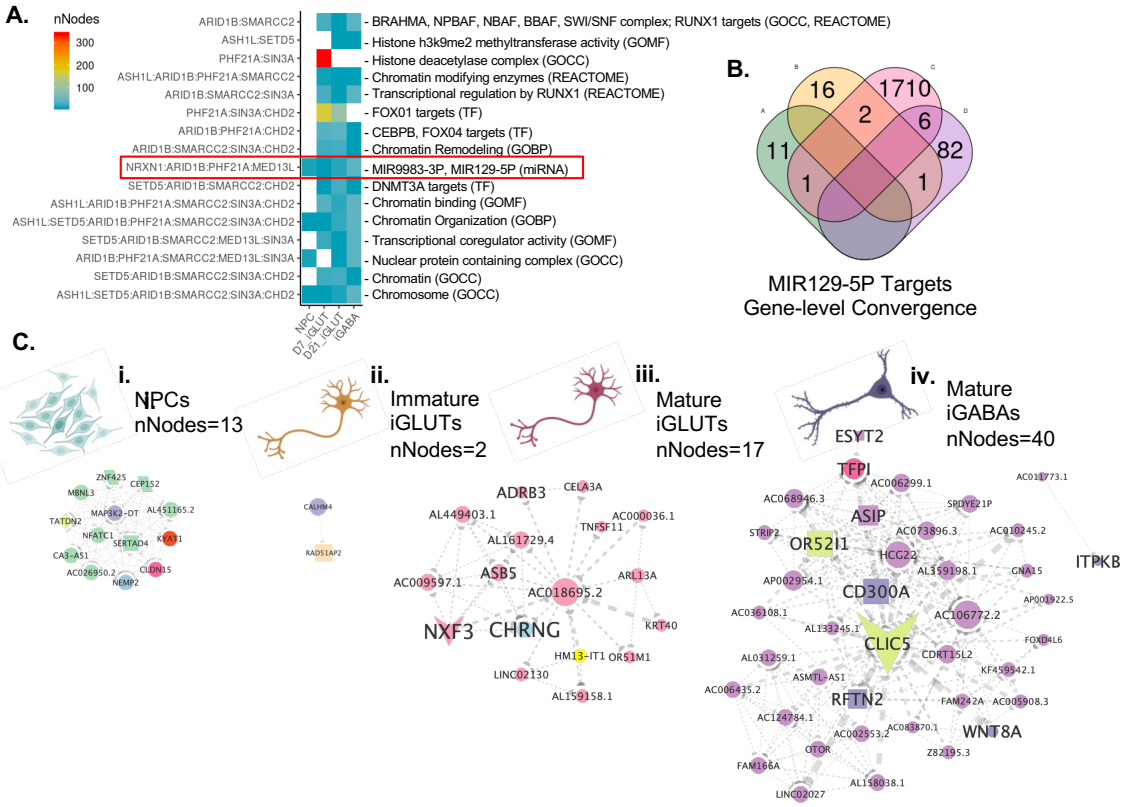

SI Fig 14. miRNA targets converge on unique networks in iNPCS, immature and mature iGLUTs, and mature iGABAs. (A) Functional gene annotation (FUMA) identified sets of KOs with shared function and shared regulation by transcription factor and miRNAs. Network convergence across KOs based on functional annotation showed cell-type specificity and resolved networks with variable convergence and gene membership **(B)** Gene-level convergence across these ASD KOs demonstrated the larges degree of convergence in glutamatergic neurons, with little overlap of convergent genes between cell-types. **(C)**.Convergent networks between targets of miRNAs MIR9983-3P and MIR129-5P (*NRXN1, ARID1B, PHF21A, MED13L*) were across all cell types, but were unique across **(i)** iNPCs. **(ii)** immature and **(iii)** mature iGLUTs and **(iv)** iGABAs. Central nodes in immature and mature iGLUTs included non-overlapping gene targets of psychiatric common and rare variants.

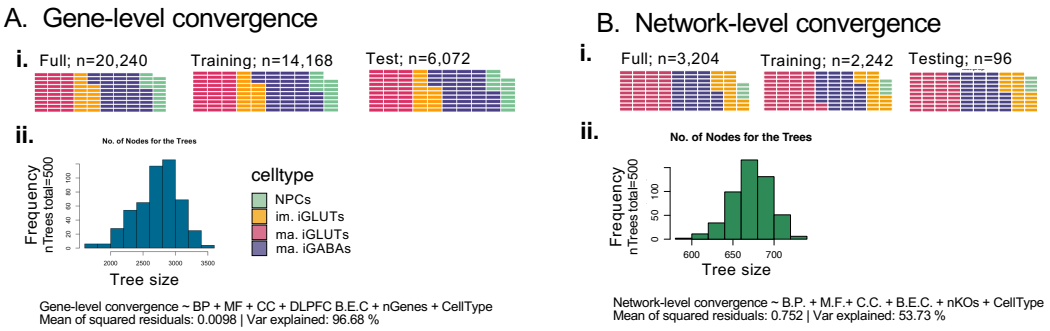

C. Number of unique ASD KO combinations tested for gene and network-level convergence

Cell-Type	# random network combinations tested (n2-10 KOs)	# network combinations resolved (n2-10 KOs)	# random gene-level combinations tested (n2-5 KOs)
NPCs	900	149	2724
Immature iGLUTs	900	594	3458
mature iGLUTs	1800	1314	6150
mature iGABAs	1800	1150	7906

SI Fig 15. Random forest training data characteristics and node frequency across trees. (A-B) Functional similarity, brain co-expression, cell-type, and the number of KOs assayed strongly predicted gene-level convergence (97% variance explained; mean of squared residuals<0.01) and moderately predicted network-level convergence (54% variance explained; mean of squared residuals=0.75). Correlation of predictor variables and gene-level **(A,i-B,i)** The proportion of cell-types is balanced across the training sets and the testing sets and is representative the full data. **(A,ii-B,ii)** Number of nodes per tree in the random forest models (nTrees total =500). C. Number of unique ASD KO combinations tested for gene and network-level convergence and used for random forest predictions. (***B.P score*** = semantic similarity of gene ontology (GO): Biological Process membership between KO genes; ***C.C. score*** = semantic similarity of GO: Cellular Component membership between KO genes; ***M.F score*** = semantic similarity of GO: Molecular functions membership between KO genes; ***B.E.C*** = dorsolateral prefrontal cortex expression correlations between KO genes; ***nKOs*** = number of KO genes tested for convergence).